Clays and Clay Minerals, Vol. 58, No. 3, 294–310, 2010.

ULTRAFINE CLAY MINERALS OF THE PLEISTOCENE OLORGESAILIE FORMATION, SOUTHERN KENYA RIFT: DIAGENESIS AND PALEOENVIRONMENTS OF EARLY HOMININS

DANIEL M. DEOCAMPO[1], ANNA K. BEHRENSMEYER[2], AND RICHARD POTTS[3,4]

[1] Department of Geosciences, Georgia State University, Atlanta, GA 30302, USA
[2] Department of Paleobiology, National Museum of Natural History, Smithsonian Institution, Washington, D.C., 20013-7012, USA
[3] Human Origins Program, National Museum of Natural History, Smithsonian Institution, Washington, D.C., 20560-0112, USA
[4] National Museums of Kenya, Department of Earth Science, Paleontology Section, Nairobi, Kenya

Abstract—The Pleistocene Olorgesailie Formation in the southern Kenya Rift has yielded a remarkable assemblage of Acheulean artifacts and vertebrate fossils, including hominin specimen KNM-OG 45500. Members 1 and 7 both contain clay-rich deposits that have been pedogenically modified into paleosols (UM1p and UM7p, respectively). This study provides the first detailed mineralogical and geochemical analyses of the clays of this important Pleistocene basin. The smectitic clays, which show abundant evidence for pedogenesis, were apparently originally deposited under lacustrine conditions. They have an average structural formula of $(Ca_{0.01}Na_{0.32}K_{0.26})(Si_{3.76}Al_{0.24})(Al_{0.86}Ti_{0.04}Fe_{0.68}Mg_{0.42})O_{10}(OH)_2$. The high layer charge clays indicate diagenetic alteration of detrital clay derived from the volcanic drainage basin, probably involving alkaline waters of variable salinity. Despite overall lower salinity compared to other Plio–Pleistocene basins of the region (*e.g.* Olduvai Gorge), the basin still shows evidence for authigenic clay mineral precipitation. Clay chemistry and bulk geochemical indicators of pedogenesis imply that UM1p clays more closely reflect depositional paleo-waters, whereas UM7p clays have been more pedogenically altered due to subaerial exposure. UM1p smectites show some Mg enrichment near the western Lava Hump locality, consistent with discharge of Mg-bearing paleo-waters from a volcanic aquifer into a siliceous and alkaline (though not highly saline) paleo-lake. UM7p smectites were deposited in a more saline paleo-lake, but have lost substantial amounts of Mg due to post-depositional weathering. Locally abundant artifacts and vertebrate fossils found in these deposits accumulated at times following deposition of the lacustrine clay, probably concurrent with pedogenesis. The limnological conditions associated with initial clay deposition, therefore, preceded hominin occupation of the exposed surfaces.

Key Words—Authigenic Clay, East Africa, Hominin, Olorgesailie, Rift Basin, Smectite.

INTRODUCTION

Background

Efforts to reconstruct aspects of East African Quaternary paleoenvironments are presently driven by the needs for (1) quantitative continental paleoclimate records, and (2) the context of evolution of hominins, other vertebrates, and their behaviors. Paleolimnological investigations are central to these efforts because lakes and paleolakes are among the most abundant and continuous sources of sedimentary data in and around the East African Rift (Ashley and Renaut, 2002).

Quantitative paleolimnological datasets have been derived from some of the larger lakes of the region, such as Lake Malawi (*e.g.* Cohen *et al.*, 2007). Some of these investigations have yielded detailed records with multi-proxy datasets based on calcareous or siliceous microfossils and pollen (Kiage and Liu, 2006) and the records have been valuable for both regional paleoclimate reconstruction and correlation with models of global paleoclimate, although most span only late Pleistocene to historic time periods. Recent work on authigenic clay minerals and other silicates suggests that these minerals can be valuable sources of time-series paleolimnological data, especially where other proxies are only present intermittently (Hay and Kyser, 2001; Deocampo, 2004; Deocampo *et al.*, 2009).

One of the best known examples of basins that produced authigenic silicates is the Late Pliocene to early Pleistocene Olduvai Gorge paleolake in northern Tanzania (Hay, 1976; Hay and Kyser, 2001). Upland weathering of reactive volcanic ashes of the basin yielded silica-rich alkaline waters, which, upon evaporative concentration within the basin, produced an assemblage of authigenic silicates including zeolites, clay minerals, K-feldspar, and Na-silicates. Authigenic clay minerals make up a large proportion of the Olduvai sediment, having formed from saline and alkaline waters under highly evaporative conditions (Deocampo *et al.*, 2002; Deocampo, 2004; Hover and Ashley, 2003; Deocampo *et al.*, 2009). Due to the rarity of calcareous and siliceous microfossils at Olduvai, the clays provide the only quantitative geochemical proxies in the basin,

* E-mail address of corresponding author:
deocampo@gsu.edu
DOI: 10.1346/CCMN.2010.0580301

i.e. stable oxygen isotopic composition (Hay and Kyser, 2001) and the amount of octahedral Mg in the clays (Deocampo, 2004; Deocampo *et al.*, 2009).

Authigenic lacustrine clays are well known from many other basins, most of which are similarly saline and alkaline and include the evaporative Lake Chad basin (Tardy *et al.*, 1974), Neogene paleolakes of France and Spain (Calvo *et al.*, 1999), alkaline volcanic basins of the Pacific Northwest (Banfield *et al.*, 1991), and arid basins of the American Great Basin (*e.g.* Jones and Spencer, 1999; Larsen, 2008).

Whether such minerals may form in fresher-water settings is an open question. Thermodynamically, certain dioctahedral smectites are favored to precipitate even in dilute waters, as long as sufficient silica is present (Jones, 1986; Deocampo, 2005), but these have not been widely reported, perhaps because detrital or biogenic materials tend to dominate freshwater deposits. If authigenic clay minerals are forming in fresher-water environments, they could represent another potentially valuable paleolimnological tool for multi-proxy studies of ancient lake deposits. This is an especially timely issue, as plans are developing for international scientific drilling in several clay-rich East African paleolakes (Cohen *et al.*, 2009; National Academy of Sciences, 2010).

The purpose of the present study was to test the hypothesis that authigenic clay minerals are present in the archaeologically significant deposits of the Olorgesailie Formation, despite the relatively fresh paleo-water chemistries suggested by the sedimentology and diatom floras. The results suggest that even in siliceous and diatomaceous sediment, authigenic clays can provide valuable perspectives on the chemistry of paleo-waters, and paleochemical variability across space and time. The study lays the groundwork for future, more detailed work in the Olorgesailie Basin, as well as other basins the authigenic clays of which have not been examined because the paleowaters were presumed to be too fresh to produce such clays.

Clay minerals in East African lakes

Many Neogene lakes and paleolakes in East Africa have developed along reaches of the East African Rift with internal drainage on down-faulted crustal blocks (Baker, 1986) and are, therefore, in many cases either hydrologically closed basins themselves or through-flow basins upstream of a terminal, evaporative lake (Jones and Deocampo, 2003). The semi-arid climate in much of East Africa has allowed many of these basins, for at least some of their histories, to achieve significant evaporative concentration of waters. The most extreme example in the region is the Natron-Magadi Basin (Figure 1), which hosts modern waters that at times exceed 300 g/kg total dissolved solids (Jones *et al.*, 1977). Such environments can, of course, change dramatically over geologic time, as demonstrated by freshwater stromatolites encrusting the rift scarp at elevations 50 m above the modern highly saline Lake Natron (Icole, 1990).

Clearly, elevated salinity and alkalinity are required for authigenic precipitation of Mg-rich clay minerals (Jones, 1986; Stoessell, 1988) and several possible mechanisms have been proposed, some of which may also occur in less saline waters. Typically, pedogenic Al-rich dioctahedral clays form through hydrolytic weathering of silica-rich glass to yield siliceous, dilute alkaline fluids (Banfield *et al*., 1991; Jones and Deocampo, 2003). The detrital source clays interact later with evaporatively concentrated fluids, yielding 'reverse hydrolysis' and neoformation of clay minerals. Several mechanisms have been proposed, including topotactic growth of interstratified kerolite ($Mg_3Si_4O_{10}[OH]_2)\cdot H_2O$) (Jones, 1986), precipitation of Mg-rich interstratifications on Al-rich substrates (Banfield *et al.*, 1991; Çolak *et al.*, 2000), and wholesale dissolution-precipitation (Hover and Ashley, 2003). At Olduvai, high-resolution transmission electron microscopy (HRTEM) studies have yielded evidence of both solid-state and dissolution-precipitation reaction mechanisms (Hover and Ashley, 2003; Deocampo *et al.*, 2009). Uptake of magnesium and silicon into authigenically precipitating clay minerals tended to increase as carbonate precipitation increased aqueous Mg/Ca, perhaps even producing pure magnesium silicate under certain conditions (Stoessell and Hay, 1978; Jones, 1986; Jones and Deocampo, 2003). The processes are strongly affected by local conditions such as the availability of Al-rich substrates to facilitate topotactic (*i.e.* template) interstratification (Jones, 1986). Trioctahedral phases have been identified in the Olduvai deposits, and detailed X-ray diffraction (XRD) and infrared spectroscopy (IR) analyses have shown that an authigenic phase of intermediate dioctahedral-trioctahedral composition has also formed there (Hover and Ashley, 2003; Deocampo *et al.*, 2009).

Evidence of Mg-enrichment in authigenic clays is best seen through calculation of structural formulae based on microanalysis of ultrafine (sub-micron) size fractions. At Olduvai this is seen clearly in the octahedral compositions of the clays (Hay and Kyser, 2001; Deocampo, 2004); whether such variation would be expected in a fresher-water paleolake such as Olorgesailie is not known. Electron microprobe analysis (EMPA) or even TEM techniques used for these microanalyses integrate a great many crystals, thus producing a 'bulk' or average geochemical signature.

Geologic setting

The deposits of the Olorgesailie Formation in southern Kenya (Figures 1b, 2) are a succession of fluviolacustrine sediments comprising diatomaceous silts and clays, some diatomite, volcaniclastic sands and gravels, and tuff (Isaac, 1978; Shackleton, 1978; Owen and Renaut, 1981; Potts *et al.*, 1999; Behrensmeyer *et al.*, 2002). Olorgesailie is famous for its abundance of well

https://doi.org/10.1346/CCMN.2010.0580301 Published online by Cambridge University Press

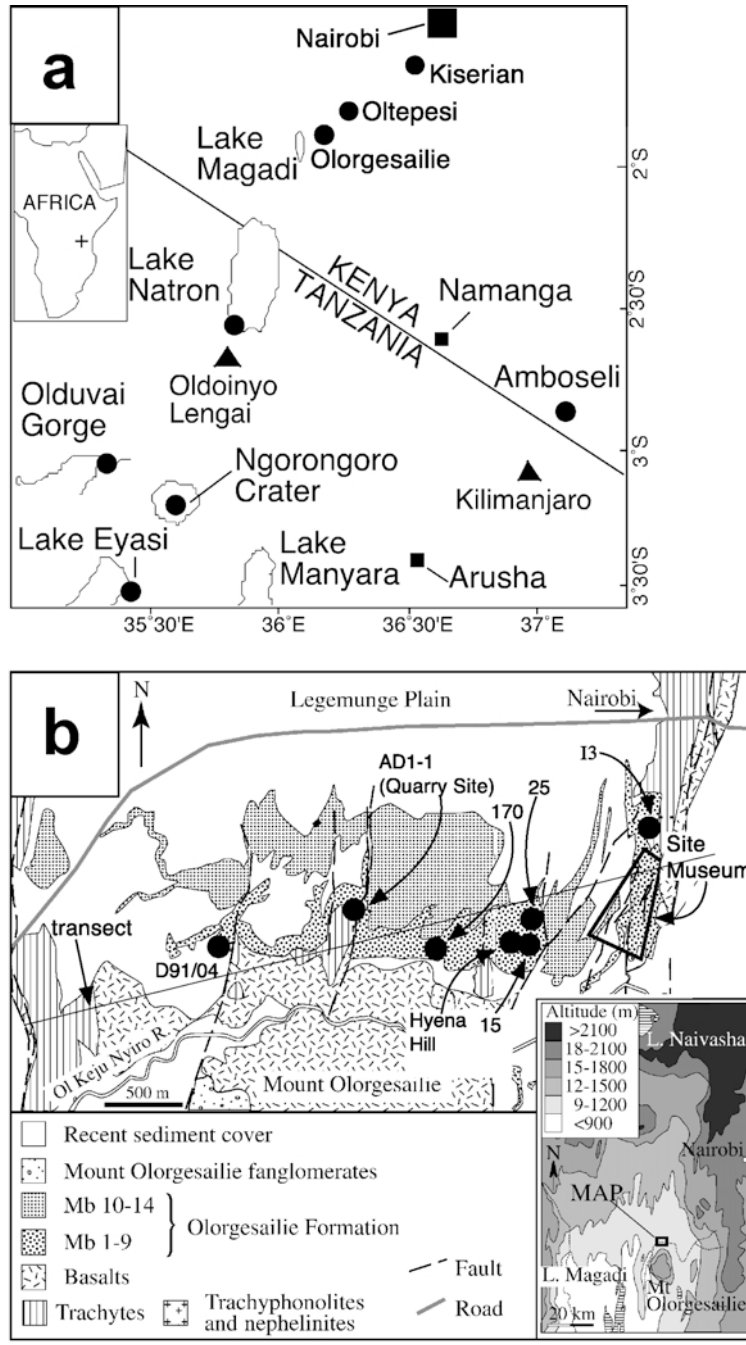

Figure 1. (a) Locations of the field areas mentioned in the text. (b) Map (Reprinted from *Palaeogeography, Palaeoclimatology, Palaeoecology*, **269**, Owen *et al.*, Diatomaceous sediments and environmental change in the Pleistocene Olorgesailie Formation, southern Kenya Rift Valley, pp. 17–37. Copyright (2008), with permission from Elsevier.) of major localities with Olorgesailie Formation outcrops and excavations, with location of the Olorgesailie Basin and other major features of the southern Kenya Rift Valley inset. Because of space limitations, only a few significant archaeological excavations are labeled. For detailed site locations, refer to Potts *et al.* (1999). Transect refers to data plotted in Figure 9.

preserved Pleistocene stone tool artifacts and associated fossil fauna (Isaac, 1977; Koch, 1986; Potts, 1989), including an ~1 my old cranium of a likely *Homo erectus* individual (KNM-OG 45500; Potts *et al.*, 2004). Efforts are underway to understand how the spatial distribution of fossils and artifacts relate to paleo-environmental features and change through time (Potts *et al.*, 1999; Sikes *et al.*, 1999; Behrennsmeyer *et al.*, 2002).

https://doi.org/10.1346/CCMN.2010.0580301 Published online by Cambridge University Press

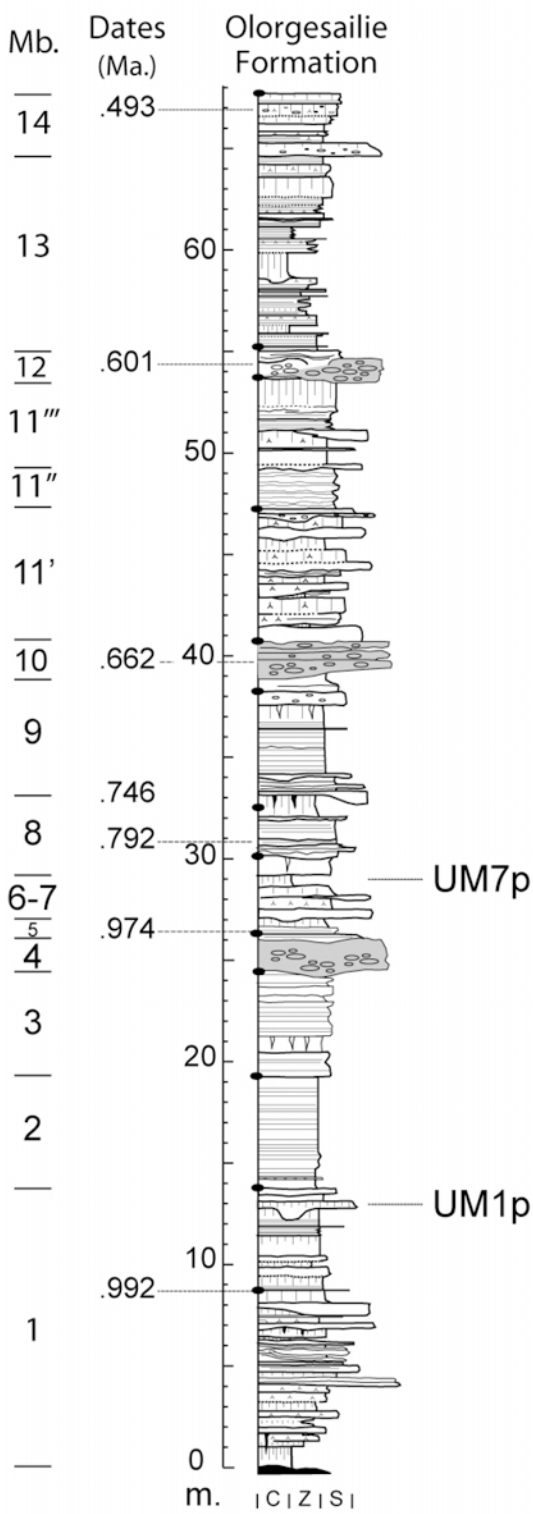

Figure 2. Composite stratigraphic section of the Olorgesailie Formation from Behrensmeyer (Owen *et al*., 2008). The target strata of this investigation are Upper Member 1 Paleosol (UM1p) and Upper Member 7 Paleosol (UM7p).

The Olorgesailie basin formed as a result of Plio-Pleistocene subsidence within the southern Kenya Rift, coincident with basin segmentation due to volcanism and block faulting (Baker and Mitchell, 1976; Baker, 1986). The Olorgesailie Formation is divided into 14 members, comprising up to 80 m of sediment which overlies unconformably an irregular lava surface (Isaac, 1978). The development of multiple horst and graben structures and southward-dipping basin tilting continued during, and following, deposition, creating a structurally complex setting (Owen and Renaut, 1981; Behrensmeyer *et al.*, 2002). Basement rocks of the basin consist mostly of basalts and trachytes, with minor phonolites associated with Mt. Olorgesailie itself (Shackleton, 1978). Continued post-depositional faulting has allowed incision along an east–west transect following the strike of the Ol Keju Nyiro River (Figure 1b), with additional exposures extending northward along several faults. Single-crystal $^{40}Ar/^{39}Ar$ dating of anorthoclase in pumice gravels and ash beds within the Olorgesailie Formation suggest sedimentation at between ~1.2 and 0.5 my ago (Figure 2; Deino and Potts, 1992).

Two intervals within Members 1 and 7 have been the foci of long-term paleontological, archeological, and paleo-environmental studies (Potts *et al.*, 1999); they are estimated to be ~0.99–0.97 and 0.78–0.75 my old, respectively (Figure 2). The Member 1 interval, known as UM1p (Upper Member 1 paleosol), is 10–30 cm thick, consists mostly of greenish-brown mudstones, with locally abundant rootmarks, slickensides, vertebrate traces, fossil bone, and stone artifacts (Potts, 1989, 1994; Potts *et al.*, 1999). The Member 7 interval, known as UM7p (Upper Member 7 paleosol), ranges from 5 to 40 cm thick, comprises greenish mud to clay, and also contains locally abundant rootmarks and slickensides. Fossils and artifacts are found within both intervals, but overall artifact densities are greater in UM1p, as will be discussed below (Potts *et al.*, 1999). Hominin specimen KNM-OG 45500 was discovered in a fluvial component of basal Member 7 (Figures 1b, 2; Potts *et al.*, 2004).

MATERIALS AND METHODS

Sampling and clay extraction

Sediment was sampled from the center of UM1p and UM7p in measured sections and sealed in polyethylene bags for transport and storage. To separate the clays, ~100 g of moist sample was soaked in ~200 mL of distilled water. Several drops of concentrated sodium hexa-metaphosphate solution were added to aid disaggregation, so Na-saturation of exchangeable sites can be assumed. Sample slurries were then centrifuged using a Sorvall Superspeed and a Beckman Ultracentrifuge at progressively higher speeds up to 40,000 rpm to isolate ultrafine, clay-size fractions following the centrifugation equations described by Jackson (1969). Almost all analyses reported here are from <0.1 μm size fractions;

https://doi.org/10.1346/CCMN.2010.0580301 Published online by Cambridge University Press

Table 1. Average chemical composition (wt.%) of <0.1 μm Olorgesailie clays determined by EMPA. Each reported value consists of five microprobe analyses for each sample, renormalized and averaged. The average standard deviation for each element (for each sample) is Na_2O = 0.4%, K_2O = 0.4%, CaO = 0.1%, MgO = 0.3%, SiO_2 = 0.8%, Al_2O_3 = 0.3%, TiO_2 = 0.2%, and Fe_2O_3 = 0.8%. Averages are shown in this table, but all individual analyses are shown in Figures 5–8. A small number of significant archeological sites is labeled in Figure 1; for more detailed location information, see Potts *et al.* (1999) and Sikes *et al.* (1999).

Sample #	Unit	Archaeological site	Na_2O	K_2O	CaO	MgO	Al_2O_3	SiO_2	TiO_2	Fe_2O_3
OG-1	UM1p	Site 25	2.5	3.2	<0.10	5.2	13.5	60.7	0.6	14.3
OG-3	UM1p	Site 21	2.2	3.4	0.19	4.8	13.9	60.9	1.1	13.5
OG-5 (<0.03μm)	UM1p	Site 15A	3.4	2.4	0.30	4.4	15.0	60.2	0.9	13.3
OG-5 (<0.1μm)	UM1p	Site 15A	2.8	3.2	0.43	4.0	14.7	60.2	1.0	13.5
OG-8	UM1p	Site 15 (mid)	2.2	2.9	0.18	3.7	14.8	59.6	0.8	14.8
OG-17	UM1p	Site 12	1.9	2.9	0.45	4.8	13.7	61.1	0.8	13.4
OG-23	UM1p	Site 3	2.5	3.6	<0.10	4.3	15.3	59.0	0.9	14.4
OG-24	UM1p	Site 118	2.2	4.2	0.13	4.2	14.2	59.9	0.8	14.3
OG-27	UM1p	Site 140D (up)	3.0	3.5	<0.10	4.3	13.9	59.7	0.9	14.6
OG-36	UM1p	Site 140G south	2.3	4.2	0.10	4.3	14.1	58.6	1.0	15.2
OG-37	UM1p	Site 155	2.9	3.4	0.17	5.0	14.1	60.0	0.8	13.5
OG-38	UM1p	Site 170	2.4	3.7	0.50	4.4	14.0	59.6	1.0	14.4
OG-39	UM1p	I-3	3.2	3.4	0.18	4.7	14.3	61.5	0.8	12.5
OG-52	UM1p	Site 93	3.4	2.5	0.16	4.0	15.0	60.9	0.8	13.0
OG-53	UM1p	Hyena Hill (lay4)	3.0	3.1	0.20	3.9	14.3	59.6	0.9	14.7
OG-67	UM1p	A-west	2.3	3.0	0.66	4.1	14.9	60.4	0.8	13.7
OG-68	UM1p	LocAquarry	2.9	2.2	0.12	8.0	13.2	59.9	0.6	12.9
OG-85	UM1p	D-91-03/4	3.8	1.7	0.33	7.5	12.7	61.7	0.6	11.7
OG-128	UM1p	D-7-1	2.9	3.8	<0.10	5.3	14.5	58.0	0.6	14.7
OG-91	UM7p	B-96-01	2.5	3.1	<0.10	2.8	16.7	57.3	0.9	16.6
OG-92	UM7p	P-10	3.5	3.1	<0.10	3.4	15.4	57.4	0.6	16.6
OG-99	UM7p	C-97-14	2.4	3.7	<0.10	3.7	15.9	57.2	0.6	16.4
OG-116	UM7p	A-96-03	1.6	3.9	<0.10	6.2	10.5	57.4	0.6	19.5
OG-119	UM7p	A-91-02	2.8	4.5	<0.10	3.9	14.6	57.4	0.8	15.9
OG-121	UM7p	91-06	2.3	3.8	<0.10	4.2	15.7	58.4	0.8	13.1
OG-122	UM7p	AD-98-2	2.3	4.2	<0.10	4.3	15.9	58.0	1.1	14.3
OG-123	UM7p	AD-97-1	2.0	4.3	<0.10	4.6	15.8	58.3	0.9	13.9
OG-129	UM7p	D-7-1	2.0	4.3	<0.10	8.5	12.2	58.8	0.9	13.2
OG-131	UM7p	D-98-3	3.3	3.1	<0.10	3.8	16.2	59.2	0.8	13.4
OG-133	UM7p	ADstop27	2.4	3.3	<0.10	6.3	14.9	59.4	0.5	13.1
OG-97	M1	I-3south	2.5	1.6	0.31	3.3	17.4	58.1	0.8	15.8
OG-98 (n = 3)	M1	C-01-01	2.8	1.7	<0.10	3.6	16.5	57.9	0.6	16.3
OG-125	M13	A94/04	2.8	2.3	<0.10	3.0	18.5	59.0	0.7	13.6
OG-137 (n = 6)	Modern	Kiserian	0.1	0.5	0.73	0.47	33.7	50.9	0.7	12.6

some are from <0.03 μm fractions (Tables 1, 2). This size separation is a crucial step in the clay purification in order to remove volcanic glass shards and diatom fragments that disrupt proper clay mineral orientation on XRD mounts (Moore and Reynolds, 1997; Deocampo, 2004). Very poor diffraction patterns were found in these samples when only <2.0 μm size fractions were extracted, leading to the erroneous conclusion that only amorphous phases are present.

Analytical methods

Samples were mounted oriented on glass slides, both air-dried and ethylene glycol solvated, following Moore and Reynolds (1997) and analyzed by XRD using CuKα radiation. Selected powders of samples were air-dried, mounted randomly oriented, and scanned from 55 to 65º2θ with very slow scan speeds to identify the 060 peaks. Sample separates were dried into pellets at 105ºC overnight, mounted in epoxy resin, polished with anhydrous lubricants, and analyzed repeatedly for major-element concentrations with a JEOL electron microprobe using wavelength-dispersive spectra, an accelerating voltage of 15 kV, and a beam current of ~5.8 nA. Shrinking of the clay extracts upon drying creates a hard clay chip that behaves mechanically like large mica grains; hence, little or no penetration of the

https://doi.org/10.1346/CCMN.2010.0580301 Published online by Cambridge University Press

Table 2. Average structural formulae of <0.1 μm Olorgesailie clays, based on the EMPA of Table 1, calculated on an $O_{10}(OH)_2$ basis, following Moore and Reynolds (1997). Elemental abundances are reported as atoms per formula unit, and charges are reported as equivalents per formula unit. Note that Sample OG-137 was found to have a heterogeneous phase composition; therefore, the calculated structural formula is only intended to show qualitative contrast to the Olorgesailie basin clays, not the true crystal composition.

Sample #	Unit	Site	Si^{TET}	Al^{TET}	Al^{OCT}	Mg^{OCT}	Fe^{OCT}	Ti^{OCT}	Na^{INT}	K^{INT}	Ca^{INT}	$Charge^{TET}$	$Charge^{OCT}$	Layer charge
OG-1	UM1p	Site 25	3.81	0.19	0.81	0.48	0.68	0.05	0.30	0.26	0.00	−0.19	−0.56	−0.75
OG-3	UM1p	Site 21	3.81	0.19	0.84	0.43	0.64	0.09	0.26	0.27	0.01	−0.19	−0.72	−0.91
OG-5 (<0.03)	UM1p	Site 15A	3.76	0.24	0.87	0.40	0.63	0.07	0.41	0.19	0.02	−0.24	−0.69	−0.93
OG-5 (<0.1)	UM1p	Site 15A	3.77	0.23	0.86	0.37	0.64	0.08	0.34	0.27	0.03	−0.23	−0.74	−0.97
OG-8	UM1p	Site 15 (mid)	3.74	0.25	0.86	0.35	0.72	0.06	0.27	0.29	0.01	−0.26	−0.58	−0.83
OG-17	UM1p	Site 12	3.83	0.17	0.86	0.44	0.64	0.06	0.23	0.24	0.03	−0.17	−0.61	−0.77
OG-23	UM1p	Site 3	3.70	0.30	0.84	0.40	0.70	0.07	0.31	0.30	0.00	−0.30	−0.59	−0.88
OG-24	UM1p	Site 118	3.77	0.23	0.84	0.39	0.69	0.06	0.27	0.35	0.01	−0.23	−0.64	−0.87
OG-27	UM1p	Site 140D (up)	3.75	0.25	0.80	0.40	0.71	0.07	0.36	0.29	0.00	−0.25	−0.70	−0.95
OG-36	UM1p	Site 140G south	3.71	0.31	0.76	0.39	0.73	0.08	0.28	0.35	0.01	−0.29	−0.66	−0.95
OG-37	UM1p	Site 155	3.77	0.23	0.82	0.46	0.61	0.06	0.35	0.29	0.01	−0.23	−0.67	−0.90
OG-38	UM1p	Site 170	3.76	0.27	0.80	0.40	0.70	0.07	0.29	0.30	0.04	−0.24	−0.69	−0.94
OG-39	UM1p	I−3	3.79	0.21	0.86	0.43	0.60	0.06	0.39	0.28	0.01	−0.21	−0.74	−0.95
OG−52	UM1p	Site 93	3.80	0.20	0.91	0.37	0.62	0.06	0.41	0.20	0.01	−0.20	−0.67	−0.87
OG−53	UM1p	HyenaHill (lay4)	3.74	0.26	0.82	0.36	0.71	0.07	0.37	0.26	0.01	−0.26	−0.69	−0.95
OG-67	UM1p	A-west	3.77	0.23	0.88	0.38	0.65	0.05	0.28	0.25	0.04	−0.23	−0.64	−0.88
OG−68	UM1p	LocAquarry	3.74	0.26	0.73	0.73	0.63	0.05	0.36	0.18	0.01	−0.26	−0.48	−0.74
OG-85	UM1p	D-91-03/4	3.83	0.17	0.77	0.68	0.56	0.05	0.45	0.14	0.02	−0.17	−0.66	−0.83
OG-128	UM1p	D-7-1	3.68	0.32	0.77	0.50	0.71	0.05	0.35	0.31	0.00	−0.32	−0.55	−0.87
OG-91	UM7p	B-96-01	3.62	0.38	0.88	0.26	0.80	0.07	0.30	0.25	0.00	−0.38	−0.46	−0.84
OG-92	UM7p	P-10	3.65	0.35	0.82	0.32	0.80	0.04	0.43	0.26	0.00	−0.35	−0.51	−0.86
OG-99	UM7p	C-97-14	3.63	0.38	0.83	0.35	0.80	0.05	0.29	0.31	0.00	−0.37	−0.42	−0.79
OG-116	UM7p	A-96-03	3.70	0.30	0.50	0.59	0.96	0.05	0.20	0.33	0.00	−0.30	−0.41	−0.72
OG-119	UM7p	A-91-02	3.65	0.35	0.77	0.36	0.78	0.06	0.34	0.38	0.00	−0.35	−0.64	−0.99
OG-121	UM7p	91-06	3.72	0.28	0.91	0.40	0.64	0.06	0.28	0.32	0.00	−0.28	−0.58	−0.85
OG-122	UM7p	AD-98-2	3.65	0.35	0.85	0.40	0.69	0.07	0.28	0.35	0.00	−0.35	−0.57	−0.92
OG-123	UM7p	AD-97-1	3.68	0.32	0.86	0.43	0.66	0.07	0.24	0.36	0.00	−0.32	−0.57	−0.89
OG-129	UM7p	D-7-1	3.72	0.28	0.64	0.79	0.64	0.07	0.25	0.35	0.00	−0.28	−0.60	−0.88
OG-131	UM7p	D-98-3	3.71	0.25	0.87	0.48	0.62	0.06	0.26	0.32	0.00	−0.25	−0.57	−0.82
OG-133	UM7p	ADstop27	3.72	0.28	0.83	0.58	0.63	0.04	0.30	0.27	0.00	−0.28	−0.44	−0.72
OG-97	M1	I-3south	3.63	0.37	0.92	0.30	0.76	0.07	0.30	0.13	0.02	−0.37	−0.36	−0.73
OG-98	M1	C-01-01	3.65	0.35	0.89	0.33	0.79	0.04	0.34	0.14	0.00	−0.35	−0.32	−0.67
OG-125	M13	A94/04	3.67	0.33	1.04	0.27	0.64	0.05	0.34	0.18	0.00	−0.33	−0.41	−0.74
OG-137*	Modern	Kiserian	3.12	0.88	1.58	0.04	0.59	0.03	0.01	0.04	0.05	−0.88	+0.62	−0.27

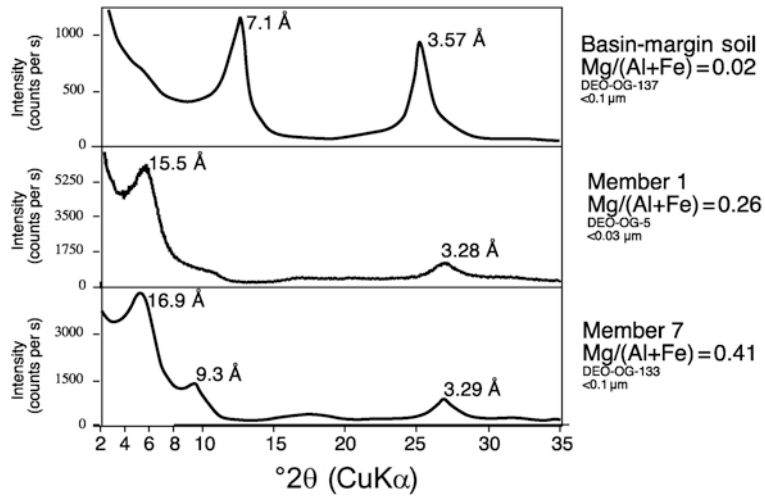

Figure 3. XRD patterns of oriented and glycolated <0.1 µm clay extracts from the basin margin soil, UM1p and UM7p. Olorgesailie clays are dominated by smectites, with little or no illitic interstratification. The Kiserian clay (OG-137) represents a modern soil from the rift highland (~20 km east of the basin), a potential analogue for detrital input into the Olorgesailie basin during the Pleistocene.

sample by epoxy was observed. All Fe was assumed to be Fe_2O_3. Analyses totaling <~90%, probably due to unintended clay rehydration, were discarded.

Structural formulae on an $O_{10}(OH)_2$ basis, including octahedral cation compositions in atoms per formula unit (a.p.f.u.), were calculated to achieve a 2:1 layer silicate structure in charge balance with 22 negative charges, following Moore and Reynolds (1997). Electrical charges for the tetrahedral and octahedral sheets were derived from the structural formulae. Although this method has been shown to have practical shortcomings in predicting cation exchange behaviors in applied settings, probably because of assumptions regarding ion behavior near exchange sites (Christidis, 2008), it remains a useful way to represent and compare compositions and crystallographic charge balance among 2:1 layer silicates (Deocampo *et al.*, 2009).

Trace metal concentrations of whole-rock powders were determined by laser ablation inductively coupled plasma mass spectroscopy (LA-ICP-MS) in the geochemistry laboratory at Michigan State University, USA. A more complete paleopedological analysis will be presented elsewhere, but selected whole-rock trace element data will be used below to test hypotheses regarding the clay geochemistry.

RESULTS

Oriented XRD

The <0.1 µm clays from both UM1p and UM7p are dominated by smectite, most with a clearly defined 17.5–18.0 Å 001 peak on glycolation, with rational basal spacings (Figure 3). Basal spacings in most samples suggest, in general, little to no illitic interlayering in the smectites. Samples from the incipient red soils on top of the eastern rift shoulder (OG-137) ~15 km to the east contain abundant kaolinite, but kaolinite was absent from all Olorgesailie samples analyzed.

Randomly oriented XRD

Measurements of the 060 peaks of randomly oriented mounts represent the average size of the clay mineral octahedral sheet (Figure 4). Local upland soil clays,

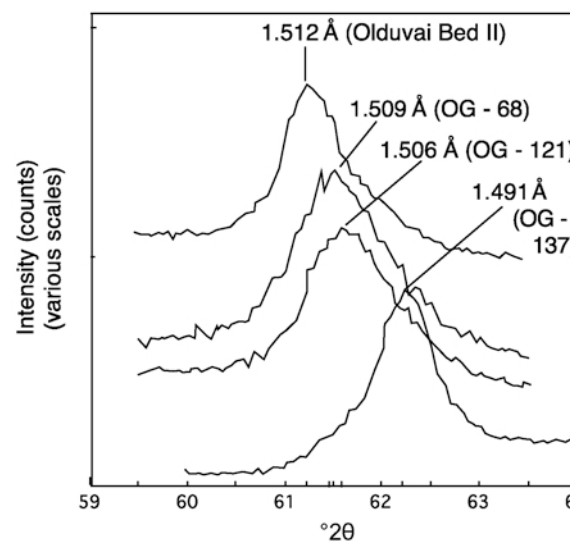

Figure 4. XRD patterns of randomly oriented <0.1 µm clay extracts from the basin margin soil and UM1p and UM7p. Peak positions are interpreted as representing average *d* space values for a mixture of somewhat homogeneous clay octahedral sheets (Moore and Reynolds, 1997). Octahedral substitution of either Fe or Mg for Al has the result of shifting the *d* space to greater values, thereby shifting the peak position to the left (Deocampo *et al.*, 2009).

https://doi.org/10.1346/CCMN.2010.0580301 Published online by Cambridge University Press

representing potential detrital source clays for the eastern margin of the basin, are easily distinguished from Olorgesailie Formation clays. The soil clays are dominated by a peak near 1.491 Å, corresponding to kaolinitic and halloysitic clays from red soils of the highland rift valley flanks. In contrast, all of the analyzed smectitic clays from within the basin have 060 peaks between 1.506 and 1.511 Å, well within the range for dioctahedral Al-rich smectite (Moore and Reynolds, 1997; Hay and Kyser, 2001).

Electron microprobe analyses

Each EMPA result used for structural calculations is the mean of 3–6 individual measurements on each sample (Tables 1, 2). Based on a total of 176 EMPA analyses, the Olorgesailie clays are nearly all purely dioctahedral (Figure 5). The analyses that plot near the border of the dioctahedral field with the "compositional gap" of Weaver and Pollard (1973) are probably due to the analytical beam including some Mg-rich crystals that are either trioctahedral (Hover and Ashley, 2003) or of intermediate dioctahedral–trioctahedral composition (Deocampo *et al.*, 2009).

The main population of octahedral compositions for samples from both members clusters around octahedral composition proportions of ~45:35:20 (Al:Fe:Mg), corresponding to an octahedral composition of ~$Al_{0.9}Fe_{0.7}Mg_{0.4}$ a.p.f.u. (Figure 6). With a majority of the charge attributable to the octahedral sheet, the smectites have a generally montmorillonitic composition (Moore and Reynolds, 1997). Significant variability is found in the octahedral composition (Figure 5), however, especially a trend toward Mg enrichment. The most Mg-rich analysis has octahedral composition proportions of 28:26:46 (Al:Fe:Mg), corresponding to a significantly enriched octahedral composition of $Al_{0.60}Fe_{0.55}Mg_{1.0}$.

Trace metals

Whole-rock Ba and Sr both vary widely (Table 3). The Ba concentrations vary from 204 to 749 mg/kg, averaging 372 mg/kg for UM1p and 395 mg/kg for UM7p. Sr concentrations vary from 50 to 229 mg/kg, averaging 123 mg/kg for UM1p and 122 mg/kg for UM7p.

DISCUSSION

Clay mineral origin and diagenesis

The clays of Members 1 and 7 examined here both occur in what have been described as "paleosols," UM1p and UM7p, respectively (Potts *et al.*, 1999). This refers to the geologic definition of a "paleosol" provided by Retallack (2001), which emphasized the alteration *in situ* of a pre-existing material at the land surface. Indeed, by this definition UM1p and UM7p are associated with abundant indicators of subaerial exposure and pedogenesis (Potts *et al.*, 1999; Sikes *et al.*, 1999; Behrensmeyer *et al.*, 2002). For UM1p, the indicators include rootmarkings, burrows, footprint surfaces, and weakly developed vertical peds. For UM7p, the indicators include prismatic to granular peds, cutans, slickensides, root traces, and root casts. Pedogenic carbonate nodules are locally common in both UM1p and UM7p (Sikes *et al.*, 1999). Because the

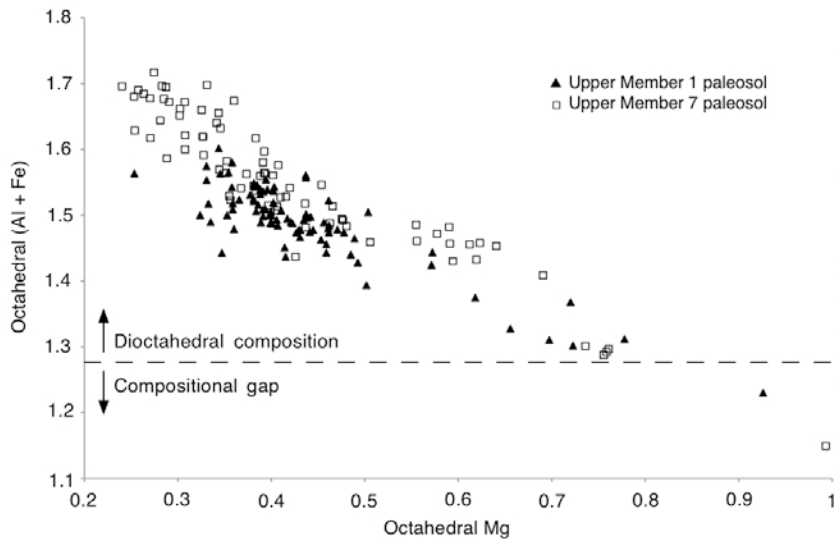

Figure 5. Octahedral cation compositions of <0.1 μm clay extracts, determined by electron microprobe analysis. (▲: UM1p samples; □: UM7p samples. Because the scale of analysis is orders of magnitude larger than individual authigenic crystals, these should be considered as averages rather than individual crystal compositions. The trend of Mg enrichment toward the "compositional gap" of Weaver and Pollard (1973), therefore, reflects clays of increasing content of either trioctahedral (Hover and Ashley, 2003) or intermediate octahedral composition (Deocampo *et al.*, 2009).

https://doi.org/10.1346/CCMN.2010.0580301 Published online by Cambridge University Press

Table 3. Whole-rock trace metal concentrations of samples from which the <0.1 μm clays were extracted, determined by LA-ICP-MS and reported as mg/kg (parts per million).

Sample #	Unit	Site	Ba	Sr	Ba/Sr
OG-1	UM1p	Site 25	336	111	3.03
OG-3	UM1p	Site 21	359	112	3.21
OG-5	UM1p	Site 15A	413	117	3.24
OG-5	UM1p	Site 15A	413	117	3.24
OG-8	UM1p	Site 15 (mid)	406	135	3.01
OG-17	UM1p	Site 12	359	106	3.39
OG-23	UM1p	Site 3	278	84	3.31
OG-24	UM1p	Site 118	433	138	3.14
OG-27	UM1p	Site 140D (up)	505	164	3.08
OG-36	UM1p	Site 140G south	341	122	2.80
OG-37	UM1p	Site 155	339	116	2.92
OG-38	UM1p	Site 170	550	229	2.40
OG-39	UM1p	I-3	239	63	3.79
OG-52	UM1p	Site 93	204	50	4.08
OG-53	UM1p	HyenaHill (lay4)	430	135	3.19
OG-67	UM1p	A-west	420	162	2.59
OG-85	UM1p	D-91-03/4	506	105	2.74
OG-128	UM1p	D-7-1	343	114	3.01
OG-91	UM7p	B-96-01	749	182	4.12
OG-92	UM7p	P-10	331	90	3.68
OG-99	UM7p	C-97-14	422	87	4.85
OG-116	UM7p	A-96-03	434	95	4.57
OG-121	UM7p	91-06	408	141	2.89
OG-122	UM7p	AD-98-2	265	100	2.65
OG-123	UM7p	AD-97-1	350	107	3.27
OG-129	UM7p	D-7-1	292	125	2.34
OG-131	UM7p	D-98-3	480	135	3.56
OG-133	UM7p	ADstop27	411	113	3.64

paleosols are very thin (<40 cm), the paleosol may not be fully diagnosed on the basis of geochemical profiles (USDA, 1999). The presence of vertical ped structures and slickensides, however, is suggestive of vertisolic paleosol development.

The UM1p and UM7p clays are unlikely to be pedogenic clays *sensu stricto*, *i.e.* the residue of hydrolytic incongruent dissolution of alumino-silicate minerals. The occurrence of these paleosols atop diatomite and diatomaceous silts does not provide suitable parent material containing abundant alumino-silicate minerals (especially feldspars or volcaniclastic glass) for strictly pedogenic production of clay minerals. In order to produce a 10−40 cm thick bed of mostly clay through pedogenic processes alone, a highly tuffaceous lithology would have to be weathered *in situ*, which would be associated with other evidence of the alteration. Instead, both glass and diatoms are preserved in the UM1p, and the diatomaceous and tuffaceous sediments of Member 7 underlying UM7p are relatively unaltered. Both of these indicate that alteration conditions were not so extreme. A simpler explanation for the origin of the clays would be as lacustrine clay, initially derived from weathering of upland volcanics in the drainage, transported into the basin, and then subjected to lacustrine early diagenesis. The relatively broad 00l peaks are consistent with lacustrine clay authigenesis, which tends to produce clay minerals with relatively low crystallinity, and even multiple authigenic phases with somewhat variable octahedral compositions (Deocampo *et al.*, 2009).

Unfortunately, the deposits are not sufficiently exposed to trace them to the basin depocenter to better characterize differential pedogenesis through the unit. Nevertheless, pedogenesis in both UM1p and UM7p was not homogeneous laterally across the units. Both UM1p and UM7p are laterally continuous, and their paleosol attributes do not cross-cut other sedimentary horizons. In that regard, the stratigraphy of these clayey deposits is consistent with lacustrine sedimentation, although pedogenic alteration is also clear. Syndepositional and post-depositional reactions have probably substantially altered the clays from their initial compositions. Upon subsequent subaerial exposure, the clays were probably also affected by pedogenesis, as discussed below, but their initial formation occurred elsewhere on the paleolandscape. In both UM1p and UM7p times, subaerial exposure occurred due to a drop in lake level, with associated minor channelization documented on these paleolandscapes (Potts *et al.*, 1999).

https://doi.org/10.1346/CCMN.2010.0580301 Published online by Cambridge University Press

The composition(s) of stream-transported, detrital clay minerals are difficult to establish. Upon entry into the complex of lake and wetland environments in the basin, they were probably chemically altered. The paleoclimate during much of the Early and Middle Pleistocene in southern Kenya was significantly more humid than present (deMenocal, 2004; Trauth *et al.*, 2005). At Olorgesailie, Sikes *et al.* (1999) also reached this conclusion based on the stable-isotope composition of paleosol carbonates. The intensity of hydrolytic weathering of volcanic rocks in the Olorgesailie drainage basin was, therefore, at least as great as at present, and probably more intense.

Clays extracted from two modern upland soils in the region have been analyzed and reported by Deocampo (2004). Both are from red soils – one developed in trachytic lava at Ngorongoro Crater, Tanzania, and the other developed on basaltic lava near Oltepesi on the flank of the southern Kenya Rift adjacent to the Olorgesailie Basin (Figure 1). Both clays were dominated by kaolinite, with minor halloysite. The clays are similar to those reported by Mahaney (1991), who analyzed late Quaternary relict soils and paleosols atop Mt. Kenya. Hay and Kyser (2001) reported a possibly Holocene illitic, pedogenic clay from the Crater wall road at Ngorongoro, again with an Al-rich octahedral composition of 1.1:0.6:0.3 (Al:Fe:Mg) a.p.f.u.

A fourth, modern clay from Kiserian was also sampled on the flanks of the Olorgesailie Basin, but at greater altitude, ~20 km to the east. Although the chemical composition was determined, structural formulae were not calculated for this clay because it is clearly heterogeneous (Table 1). The XRD results (Figures 3, 4) show it is composed of kaolinite and smectite, probably an Fe-rich smectite, considering that the bulk sample contained up to 12% Fe_2O_3. Clays in the Kiserian soil are, therefore, dominated by Al-rich and relatively Fe-rich clays with very small layer charge. The alkali cation content (*i.e.* interlayer cations) in the clay is an order of magnitude less than those of the Olorgesailie clays, with the exception of Ca^{2+}, which is to be expected because Ca^{2+} affinity is greatest for clays equilibrated with fresh waters.

Any potential detrital source clays originating in upland soils around Olorgesailie were, therefore, likely to be the products of fairly heavy weathering. As all these modern soils (which are probably less intensely weathered than those of the early Pleistocene) show, pedogenic clays in the region are more likely to be Al-rich. Even for a smectitic or illitic pedogenic clay source, clays would have been dominated by Al and Fe, with negligible octahedral substitution of Mg. Al- and Fe-dominated clays have been documented in many Holocene and younger soils of the region (Jager, 1982; Mizota *et al.*, 1988). During periods of axial drainage within the Rift, the relative proportions of such pedogenic clays in transport and reworked sedimentary clays may have varied. Without sedimentological data indicating such detrital transport, the possibility of this variation is difficult to assess.

Alternatively, much of the clay may be derived from a more pure, pedogenic smectite developed through incomplete hydrolysis in the Olorgesailie drainage basin itself. Indeed, Hover and Ashley (2003) reported similar clay compositions in Pleistocene volcaniclastic fan sediments on the western flank of the Ngorongoro Volcanic Highlands. Deocampo *et al.* (2009) argued that the same sediments also appear to have been influenced by alkaline waters in the basin, based on HRTEM observations of microfabrics, increased layer charge, and interlayer cation contents.

The compositions of the Olorgesailie clays are in contrast to these hypothetical upland pedogenic sources, with uniform 2:1 mineralogy, high layer charge dominated by the octahedral sheet, and (for a small number of samples) a Mg-enrichment trend (Table 2, Figure 6). The compositions are consistent with the formation of authigenic or diagenetic smectite and illite-smectite in standing water with elevated silica and alkali contents (Jones, 1986). Indeed, the abundant diatoms in the basin provide a ready source of amorphous silica to support clay neoformation in alkaline lake waters, perhaps similar to the dramatic transformation of diatom frustules to authigenic clay as reported from the Bolivian salars (Badaut and Risacher, 1983). Such a

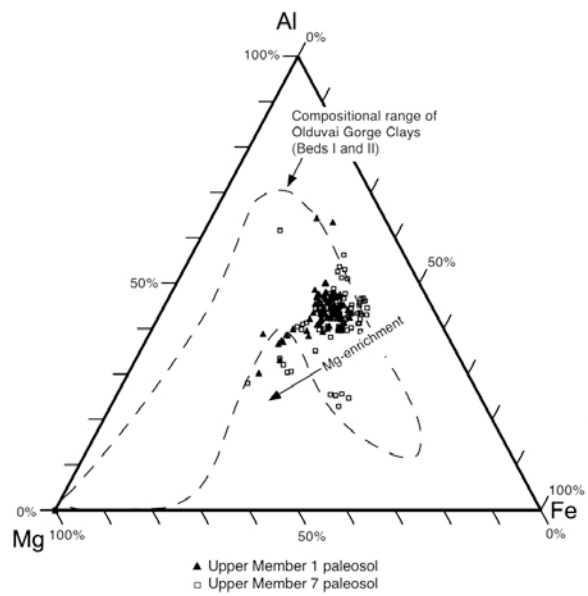

Figure 6. Ternary diagram showing trends in the octahedral-cation composition of the Olorgesailie Clays. ▲: UM1p samples; □: UM7p samples. For comparison, the approximate range of clay mineral compositions from the nearby Olduvai basin are shown (Hay and Kyser, 2001; Deocampo *et al.*, 2002; Hover and Ashley, 2003; Deocampo, 2004; Deocampo *et al.*, 2009).

https://doi.org/10.1346/CCMN.2010.0580301 Published online by Cambridge University Press

transformation does not require high salinity for most of the clays, although the Mg-rich clays were certainly formed in more concentrated waters.

Smectite layer charge

The compositional patterns are the same for both UM1p and UM7p clays – both have mostly the same compositional clustering and a small number of samples with evidence of Mg enrichment (Figures 5 and 6). One significant difference between them does exist, however – the relative contributions of the tetrahedral and octahedral sheets to the total layer charge. Increase in octahedral charge (calculated as the difference between positive charges from octahedral cations and negative

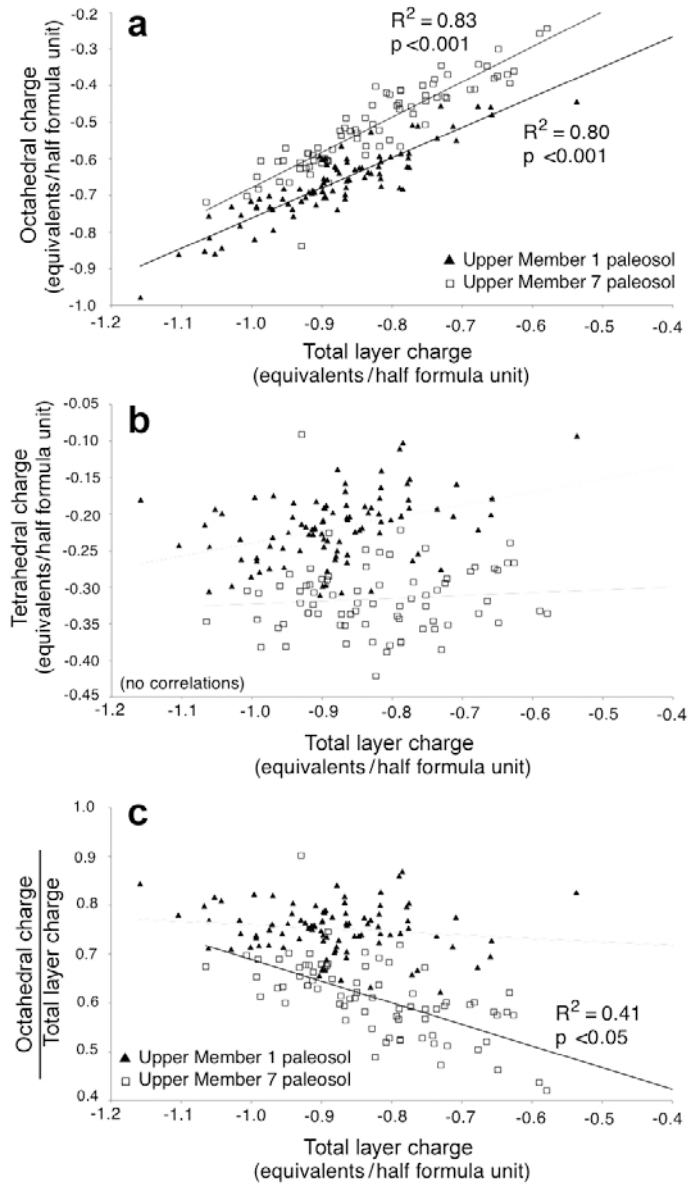

Figure 7. Layer-charge relationships for the Olorgesailie <0.1 μm clays, calculated from structural formulae based on electron microprobe analyses. ▲: UM1p samples; □: UM7p samples. Reported p values for correlations are one-tailed. (a) The relationship between octahedral charge and the total layer charge (octahedral plus tetrahedral charges) – variations in layer charge are due primarily to variations in octahedral charge. (b) The relationship between tetrahedral charge and the total layer charge – no correlations were found, again confirming the dominance of octahedral variations in controlling layer charge in these clays. (c) Relationship between the octahedral charge proportion (octahedral charge divided by total layer charge) and total layer charge. For UM1p, no relationship was found, showing that octahedral charge dominates layer charge across all values of layer charge. For UM7p, however, a good correlation was found, showing that octahedral charge dominates only for samples with high layer charge – the only significant difference found between clays of UM1p and UM7p, reflecting a difference in diagenetic history.

https://doi.org/10.1346/CCMN.2010.0580301 Published online by Cambridge University Press

charges from octahedral oxygen atoms) is the primary factor in increasing the overall layer charge for both UM1p and UM7p clays (Figure 7a), consistent with a diagenetic process primarily affecting octahedral compositions (*i.e.* Mg substitution).

The two paleosols differ, however, in the variations of the proportion of total layer charge represented by the octahedral sheet. For all UM1p samples, octahedral charge dominates but for UM7p, octahedral charge only dominates in the samples that have a large total layer charge (Figure 7c). For those UM7p samples with total layer charge of <~−0.8 equivalents per formula unit, the charge is about evenly split between octahedral and tetrahedral sheets. The patterns in layer charge appear to derive from the larger amount of Al substitution in the tetrahedral sheets for the UM7p samples (Table 2). This may be related to the greater role played by low-temperature illitization, with enhanced Al substitution, an increase in layer charge due to increased tetrahedral charge, and eventually K fixation (Eberl *et al.*, 1986, 1993). The effects of pedogenic alteration are reflected here, an hypothesis tested below through the use of trace-metal analysis. For all samples, however, changes in octahedral charge are clearly the greatest contribution to layer charge, and these are most strongly related to transformations affecting octahedral cation composition.

Another potential source of increased layer charge is the reduction of octahedral Fe(III) to Fe(II), a process common to many anaerobic depositional settings (*e.g.* Singer and Stoffers, 1980). Unfortunately, redox chemistry data are unavailable for the present samples (*i.e.* FeO/Fe_2O_3) and the reduction is not likely to be an important contributor to layer charge because no significant correlation is found between Fe content and the components of layer charge (Table 2).

Trace-metal analysis of the UM1p and UM7p bulk paleosol samples are consistent with the interpretation that pedogenesis, including hydrolytic alteration, imprinted the geochemical signature of the authigenic clays to a greater extent on UM7p than on UM1p. A strong relationship is seen between clay geochemistry and the Ba/Sr ratio of whole-rock samples. Ba/Sr ratios are commonly used in paleopedology as a geochemical proxy for the intensity of hydrolytic alteration (*i.e.* leaching) that has occurred (Retallack, 2001; Sheldon and Tabor, 2009). Because Sr is much more soluble than Ba, as hydrolytic weathering proceeds, preferential Sr loss increases the bulk Ba/Sr value. Therefore, greater Ba/Sr values indicate more leaching. In the UM1p clays, no relationship is seen between Ba/Sr and ultrafine clay chemistry (Figure 8a). In UM7p, however, a strong inverse relationship is found between bulk Ba/Sr and the proportion of layer charge in the ultrafine clays attributed to the octahedral sheet, calculated as octahedral layer charge (OC) divided by total layer charge (LC) (Figure 8b). Samples with greater bulk Ba/Sr have smaller OC/LC values, implying that, for UM7p, hydrolytic alteration due to pedogenesis has locally affected the clay geochemistry, reducing octahedral charge, and proportionally enhancing the tetrahedral charge. Clay chemistry is altered most in those samples which are most intensely leached, *i.e.* those which have the greatest Ba/Sr values. Such patterns are not seen in UM1p, suggesting that post-depositional alteration was not as severe in UM1p, and that the geochemical variation is more indicative of primary lacustrine conditions. The more common occurrence of pedogenic structures in UM7p, such as ped formation and shrink-swell slickensides, reinforce this.

Examination of the lateral variations in clay octahedral Mg content and whole-rock Ba/Sr ratios shows an

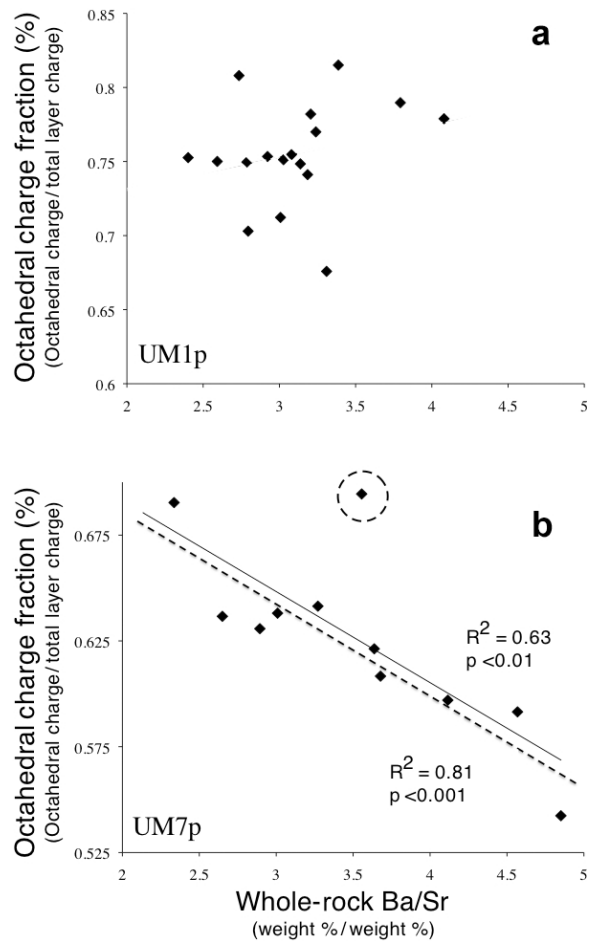

Figure 8. Relation between the octahedral charge fraction for <0.1 μm clays, averaged from all electron microprobe analyses for each sample, and the trace metal ratio Ba/Sr for the whole-rock sample, determined by laser ablation ICP-MS. Ba/Sr is an indicator of hydrolytic alteration (*i.e.* pedogenesis; Retallack, 2001; Sheldon and Tabor, 2009), which apparently had a much greater impact on UM7p clay geochemistries than on UM1p. For b, correlation coefficients are shown both for the complete dataset (solid line) and for the dataset with the outlier data point removed from the calculation (dashed line). Reported p values for correlations are one-tailed.

https://doi.org/10.1346/CCMN.2010.0580301 Published online by Cambridge University Press

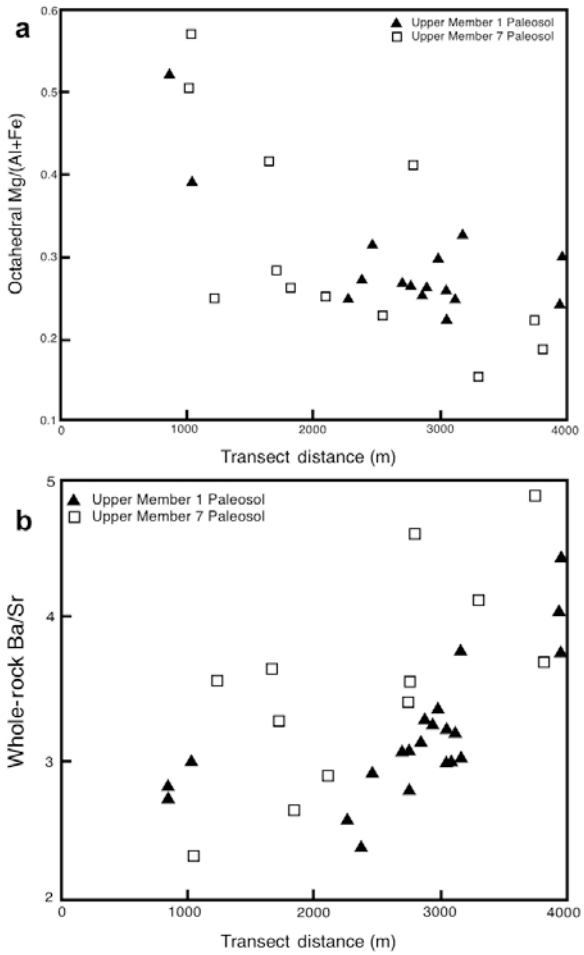

Figure 9. Lateral variation in octahedral clay chemistry and whole-rock Ba/Sr ratios along the transect plotted in Figure 1. Clay chemistry in UM1p is fairly uniform in most of the field area, with the high-Mg samples in the west. UM7p clay chemistry is more variable. Both UM1p and UM7p show eastward increases in Ba/Sr, though it is more pronounced in UM1p.

interesting comparison between UM1p and UM7p (Figure 9). The Mg content in the UM1p clays is fairly homogeneous, with the Octahedral Cation Index (Mg/(Al + Fe); Deocampo, 2004) of these clays being ~0.25–0.32 across the eastern part of the field area. Only in the extreme western samples (near the Lava Hump) do they rise considerably, as high as ~0.50. The Mg content in UM7p clay, however, is more variable, ranging from ~0.15 to 0.4 in the eastern areas, and again rising to >0.50 in the west. Because the clay Mg content is well correlated with bulk Ba/Sr in UM7p, similar lateral variations in Ba/Sr values for that unit are distributed in the same fashion. UM1p Ba/Sr values appear to rise systematically toward the east, a pattern not seen in any other geochemical indicator observed, and one not significantly related to clay chemistry. The Mg content is a topic of continuing research that will be addressed elsewhere; the behavior must be explained either by Sr depletion due to hydrolytic weathering in the east or by Sr enrichment due to alkaline deposition in the west (Figure 9b).

An alternative explanation for the Ba/Sr ratios is that carbonate-bearing groundwaters locally enriched deposits in Sr at times of carbonate precipitation. The carbonate nodules are small (0.1–1.5 cm in diameter), however, and have been interpreted not as groundwater carbonates, but rather as pedogenic carbonates (*i.e.* in equilibrium with soil CO_2; Sikes *et al.*, 1999). A pedogenic origin would, therefore, not enrich the bulk sediment in Sr. A third possibility is that aeolian input of sodium carbonate dust from other evaporative watersheds in the basin could have locally enriched the sediment in alkalis, even perhaps contributing to the carbonate nodule formation. This is a difficult hypothesis to test, however, considering how soluble the materials were and the relatively fresh paleowaters of the Olorgesailie basin.

Paleoenvironmental implications

Although the clayey deposits of UM1p and UM7p are both thin, ⩽40 cm, the laterally continuous clay-rich deposits are strongly suggestive of open-water conditions. Octahedral compositions of the clays are very similar between the two members, suggesting similar geochemical environments (Figure 6). Although a Mg-enrichment trend is apparent in some samples, even the most Mg-rich have octahedral Mg of only ~1.0 a.p.f.u., good evidence for diagenesis in alkaline lake water (Jones, 1986), although perhaps of only moderate salinity (Deocampo, 2004). By way of comparison, expansion of Paleolake Olduvai ~1.8 my ago was recorded by a change in authigenic clay mineral octahedral Mg content from ~2 at lowstand to ~1 a.p.f.u. at high stand (Deocampo, 2004). Mg-enrichment in the Olduvai clays appears to be due to solid-state alteration to an illite-smectite with intermediate octahedral composition (Deocampo *et al.*, 2009) or trioctahedral illite (Hover and Ashley, 2003). Such alteration requires a diagenetic environment with pore fluids with elevated salinity and high Mg/Ca ratios. K-fixation may have occurred contemporaneously or later. No HRTEM investigations have yet been carried out on the Olorgesailie clays, but if similar processes are at work, then the Olorgesailie clays with the greatest Mg content represent paleolake waters with salinities about as great as Paleolake Olduvai during freshwater times. Hay and Kyser (2001) characterized this as moderate salinity and pH <9.5. For UM1p, this is consistent with lacustrine diatom transfer functions approximating paleo-conductivity at 1000–10000 μS/cm and paleo-pH at 8.5–9.5 (Owen *et al.*, 2008). Insufficient diatoms have been found in UM7p for such a calculation.

Although the variability is not great among the samples studied here, the small number of samples that

https://doi.org/10.1346/CCMN.2010.0580301 Published online by Cambridge University Press

do show significant levels of Mg enrichment requires explanation. The variability can be explained in one of two ways. Either (1) the Mg enrichment trend is a primary feature, representing lacustrine paleoenvironmental gradients or heterogeneity, or (2) the octahedral variations reflect differential pedogenic alteration of the primary, laterally uniform composition. The first possibility is consistent with a freshwater source feeding a lake with elevated salinity; waters nearer the source (*e.g.* stream or spring discharge) would have lower salinities. Such a condition is generally seen in large, heavily evaporated lakes where very large concentration gradients lie between fresh and evolved waters. One of the first major studies of Mg enrichment in authigenic clays was just such a case, at Lake Chad. Millot (1964) found that the most Mg-rich clays were in the basin center, whereas clays at the periphery, nearer to inflow, had less Mg content. This seems unlikely for the Olorgesailie Basin, which only sporadically reached very high salinity (Behrensmeyer *et al.*, 2002; Owen *et al.*, 2008). If, however, the pattern in Mg enrichment is a primary signal of lacustrine sedimentation, then for UM1p the most Mg-rich clays are found to the west at the 'Quarry Site' (Site AD1-1) adjacent to a faulted basaltic lava known as the 'Lava Hump.' Because of the proximity to the lava, Mg enrichment may have occurred in the lake because of the influence of the lavas on groundwater chemistry. A similar setting is reported for Late Pleistocene and modern Mg-rich clays in the Amboseli basin next to Mt. Kilimanjaro, where discharging groundwaters have slightly elevated Mg content. They erupt into siliceous, alkaline waters, allowing Mg-rich clays to form without substantial evaporative concentration (Stoessell and Hay, 1978; Deocampo, 2005). Alternatively, more saline and alkaline conditions existed to the west though no gradual gradient toward greater Mg content in the west was found – only the peak in Mg content near the Lava Hump. For UM7p, no single direction in Mg enrichment was found laterally – a relatively large Mg content was found at several points throughout the basin (Figure 9). If this pattern is a primary signal from the lake, then it reflects bottom-water heterogeneity rather than a paleoenvironmental gradient.

The second scenario explaining Mg abundance is that the variations are due to secondary diagenetic and/or pedogenic alteration of original Mg-bearing clays. Such was found to be the case at Olduvai Gorge, where original primary Mg-rich clays (deposited at high lake stand) were preferentially leached of Mg in areas where surface- and groundwater-fed wetlands developed (Deocampo *et al.*, 2002). In pore waters where microbial degradation of organic matter leads to high P_{CO_2} (commonly found in wetlands), the resulting pH changes can strongly impact diagenetic mineral stabilities (Langmuir, 1997; Deocampo and Ashley, 1999). The effects on precipitation and alteration of Mg-rich clays can be significant (Deocampo, 2005). If this second scenario is the reason for lateral variability in Mg content, then high points in Mg indicate areas where clays were not leached of their Mg. The other areas (the majority of the sampled localities) would have been areas of relatively freshwater pedogenic or diagenetic conditions – areas of subaerial weathering and infiltration, wetlands, or relatively fresh lakes. The abundant pedogenic structures such as clay cutans and slickensides are most consistent with subaerial weathering. If this second scenario is correct, then the clay chemistries are more relevant for the vertebrate fossils and archeology, because they are associated with the period of pedogenesis rather than with deposition of the lacustrine clays.

Such a scenario is consistent with the findings of Trueman *et al.* (2006), who attributed the great variability over short distances in the abundances of rare earth elements in fossil bone to the heterogeneity of pore waters in soil environments. The Trueman *et al.* (2006) sampling was more dense than the sampling reported here, and those authors found significant compositional variability within Members 1 and 7 over lateral distances <10 m. Within Member 7, Trueman *et al.* (2006) found that light rare earth element (*LREE*) enrichment patterns within fossil bones suggested more reducing conditions to the west, with less reducing conditions indicated in the east. This corresponds approximately to samples OG-122 and 123 in the west, and OG-99 in the east (Tables 1–3). The Ba/Sr ratios (~4.85) and ultrafine clay Mg content (~0.35 a.p.f.u.) for these samples is consistent with shorter pore-water residence times (and hence greater leaching) in the east as compared to the west (Ba/Sr = 2.65 and 3.56, Mg_{oct} = 0.40 and 0.43 a.p.f.u.). The results suggest that bulk geochemistry, clay mineral chemistry, and bone *REE*s all indicate patterns of differential diagenesis on the paleolandscape associated with the period of pedogenesis.

The relationships between clay chemistry and whole-rock trace-element geochemistry (Figure 8) have led to the conclusion that the clay chemistries of the two paleosols formed differently. The UM1p clays reflect the primary lacustrine conditions under which the clays formed, with the only Mg enrichment occurring near a Mg-bearing groundwater source near the Lava Hump (Figure 1). In contrast, only the most Mg-rich clays of UM7p retain a geochemical signal from the original paleolake. Furthermore, because Mg-enrichment was widespread rather than due to isolated groundwater input, it was probably a more concentrated paleolake than that in which the UM1p clays were deposited. Subsequent pedogenic alteration of the clays under conditions of subaerial weathering and infiltration of fresh water has locally leached some of the clays of their Mg content, yielding the observed lateral variations in clay chemistry.

Independent estimates of the time represented by UM1p and UM7p are consistent with these inferences. Potts *et al.* (1999) used radiometric dates and rates of

https://doi.org/10.1346/CCMN.2010.0580301 Published online by Cambridge University Press

sediment accumulation to calculate a maximum time span of 1000 y for the deposition and alteration of UM1p. In contrast, UM7p occurs within a part of the Olorgesailie Formation that includes significant hiatuses, and this paleosol could represent as much as 190,000 y based on the nearest dated strata and sediment accumulation estimates (Potts *et al.* 1999, p. 774). The upper surface of UM7p is truncated by an erosional unconformity, and the actual period of soil formation was probably <190 ky but still considerably more than that of UM1p.

CONCLUSIONS

Paleosols within Members 1 and 7 of the Olorgesailie Formation contain lacustrine clay dominated by smectite that has been pedogenically altered to varying degrees. Although composition is variable, an average structural formula for these clays in charge balance is $(Ca_{0.01}Na_{0.32}K_{0.26})(Si_{3.76}Al_{0.24})(Al_{0.86}Ti_{0.04}Fe_{0.68}Mg_{0.42})O_{10}(OH)_2$. The mineralogy and geochemistry of these relatively high-charge clays is consistent with clay minerals derived initially from soils of the region, but diagenetically altered in alkaline (though not highly saline) waters of the Olorgesailie paleolake. Some significant Mg enrichment is found, but overall the samples are consistent with a fresher-water (though alkaline) paleoenvironment. Local Mg enrichment of clays near the Lava Hump in UM1p is interpreted to be the effect of paleo-groundwater discharging from volcanic aquifers into a fresh (though alkaline) paleolake. The UM7p clays were deposited in a more saline paleolake, but pedogenic alteration has apparently more strongly altered the primary lacustrine geochemical signal to a degree not seen in UM1p.

In environmental interpretations relating to hominin landscape use and paleoecology, distinguishing between primary deposition and post-depositional alteration is critical. The fresh to slightly alkaline conditions of the lakes where the UM1p and UM7p primary sediments formed preceded the time when hominins actually occupied the land surfaces formed on these deposits, emphasizing the importance of the pedogenic features of clays in distinguishing the relatively brief period of land-surface exposure of UM1p, which is extraordinarily rich in fossils and hominin traces, from the longer period of pedogenesis in UM7p, where the archeological and paleontological record is much sparser. The idea that more time should correlate with more fossils and artifacts incorporated into a paleosol is clearly contradicted by this evidence, providing additional questions for paleoanthropology regarding hominin behavior and resource utilization.

ACKNOWLEDGMENTS

Olorgesailie fieldwork is a long-term collaborative project of the National Museums of Kenya and the Human Origins Program of the Smithsonian Institution. The research reported here was supported by the Smithsonian Institution Office of Fellowships, the National Science Foundation (#0202612), the Natural History Museum, UK, and the Wenner Gren Foundation (#6764).

REFERENCES

Ashley, G.M. and Renaut, R.W. (2002) Rift sedimentation. Pp. 3–7 in: *Sedimentation in Continental Rifts* (R.W. Renaut and G.M. Ashley, editors). Special Publication **73**, SEPM (Society for Sedimentary Research), Tulsa, Oklahoma, USA.

Badaut, D., and Risacher, F. (1983) Authigenic smectite on diatom frustules in Bolivian saline lakes. *Geochimica et Cosmochimica Acta*, **47**, 363–375.

Baker, B.H. (1986) Tectonics and volcanism of the southern Kenya Rift Valley and its influence on rift sedimentation. Pp. 45–57 in: *Sedimentation in the African Rifts* (L.E. Frostick, R.W. Renaut, I. Reid, and J.J. Tiercelin, editors). Special Publication **25**, The Geological Society, London.

Baker, B.H., and Mitchell, J.G. (1976) Volcanic stratigraphy and geochronology of the Kedong-Olorgesailie area and the evolution of the South Kenya Rift valley. *Journal of the Geological Society of London*, **132**, 467–484.

Banfield, J.F., Jones, B.F., and Veblen, D.R. (1991) An AEM-TEM study of weathering and diagenesis, Abert Lake, Oregon: I, weathering reactions in the volcanics. *Geochimica et Cosmochimica Acta*, **55**, 2795–2810.

Behrensmeyer, A.K., Potts, R., Deino, A., and Ditchfield, P. (2002) Olorgesailie, Kenya: A million years in the life of a rift basin. Pp. 97–106 in: *Sedimentation in Continental Rifts* (R.W. Renaut and G. M. Ashley, editors). Special Publication **73**, SEPM (Society for Sedimentary Geology), Tulsa, Oklahoma, USA.

Calvo, J.P., Blanc-Valleron, M.M., Rodrigues-Arandia, J.P., Rouchy, J.M., and Sanz, M.E. (1999) Authigenic clay minerals in continental evaporitic environments. Pp. 129–151 in: *Reefs and Carbonate Platforms in the Pacific and Indian Oceans* (G.F. Camoin and P.J. Davies, editors). Special Publication **27**, International Association of Sedimentologists.

Christidis, G.E. (2008) Validity of the structural formula method for layer charge determination of smectites: A re-evaluation of published data. *Applied Clay Science*, **42**, 1–7.

Cohen, A., Stone, J., Beuning, K., Park, L., Reinthal, P., Dettman, D., Scholz, C.A., Johnson, T., King, J.W., Talbot, M., Brown, E., and Ivory, S. (2007) Ecological consequences of Early Late-Pleistocene megadroughts in tropical Africa. *Proceedings of the National Academy of Sciences*, **104**, 16422–16427.

Cohen, A., Arrowsmith, R., Behrensmeyer, A.K., Campisano C., Feibel, C., Fisseha, S., Johnson, R., Bedaso, Z.K., Lockwood, C., Mbua, E., Olago, D., Potts, R., Reed, K., Renaut, R. Tiercelin, J.-J., and Umer, M. (2009) Understanding Paleoclimate and Human Evolution through the Hominin Sites and Paleolakes Drilling Project. *Scientific Drilling*, **8**, 60–65.

Çolak, M., Helvaci, C., and Maggetti, M. (2000) Saponite from the Emet Colemanite mines, Kütahya, Turkey. *Clays and Clay Minerals*, **48**, 409–423.

Deino, A. and Potts, R. (1992) Age-probability spectra for examination of single-crystal 40Ar/39Ar dating results: examples from Olorgesailie, southern Kenya rift valley. *Quaternary International*, **7/8**, 81–89.

deMenocal, P.B. (2004) African climate change and faunal evolution during the Pliocene-Pleistocene. *Earth and Planetary Science Letters*, **220**, 3–24.

Deocampo, D.M. (2004) Authigenic clays in East Africa:

Regional trends and paleolimnology at the Plio–Pleistocene boundary, Olduvai Gorge, Tanzania. *Journal of Paleolimnology*, **31**, 1–9.

Deocampo, D.M. (2005) Evaporative evolution of surface waters and the role of aqueous CO_2 in magnesium silicate precipitation: Lake Eyasi and Ngorongoro Crater, northern Tanzania. *South African Journal of Geology*, **108**, 493–504.

Deocampo, D.M. and Ashley, G.M. (1999) Siliceous islands in a carbonate sea: Modern and Pleistocene records of spring-fed wetlands in Ngorongoro Crater and Olduvai Gorge, Tanzania. *Journal of Sedimentary Research*, **69**, 974–979.

Deocampo, D.M., Blumenschine, R.J., and Ashley, G.M. (2002) Freshwater wetland diagenesis and traces of early hominids in the lowermost Bed II (~1.8 myr) playa lake-margin at Olduvai Gorge, Tanzania. *Quaternary Research*, **57**, 271–281.

Deocampo, D.M., Cuadros, J., Wing-Dudek, T., Olives, J., and Amouric, M. (2009) Saline lake diagenesis as revealed by coupled mineralogy and geochemistry of multiple ultrafine clay phases: Pliocene Olduvai Gorge, Tanzania. *American Journal of Science*, **309**, 834–868.

Eberl, D.D., Środoń, J., and Northrop, H.R. (1986) Potassium fixation in smectite by wetting and drying. Pp. 296–326 in: *Geochemical Processes at Mineral Surfaces* (J.F. Davis and K.A. Hayes, editors), **323**, American Chemical Society Symposium Series.

Eberl, D.D., Velde, B., and McCormick, T. (1993) Synthesis of illite-smectite from smectite at earth surface temperatures and high pH. *Clay Minerals*, **28**, 49–60.

Hay, R.L. (1976) *Geology of the Olduvai Gorge*. University of California Press, Berkeley, California, USA, 203 pp.

Hay, R.L. and Kyser, T.K. (2001) Chemical sedimentology and paleoenvironmental history of Lake Olduvai, a Pliocene lake in northern Tanzania. *Geological Society of America Bulletin*, **113**, 1505–1521.

Hover, V.C. and Ashley, G.M. (2003) Geochemical signatures of paleodepositional and diagenetic environments: a STEM/AEM study of authigenic clay minerals from an arid rift basin, Olduvai Gorge, Tanzania. *Clays and Clay Minerals*, **51**, 231–251.

Icole, M. (1990) Pleistocene lacustrine stromatolites, composed of calcium carbonate, fluorite, and dolomite, from Lake Natron, Tanzania: depositional and diagenetic processes and their paleoenvironmental significance. *Sedimentary Geology*, **69**, 139–155.

Isaac, G.L. (1977) *Olorgesailie: Archaeological Studies of a Middle Pleistocene Lake basin in Kenya*. University of Chicago Press, Chicago, USA.

Isaac, G.L. (1978) The Olorgesailie Formation. Pp. 173–206 in: *Geological Background to Fossil Man* (W.W. Bishop, editor). Scottish Academic Press, Edinburgh.

Jackson, M.L. (1969) *Soil Chemical Analysis, Advanced Course*. Published by the author, Madison, Wisconsin, USA.

Jager, T.J. (1982) *Soils of the Serengeti Woodlands, Tanzania*. Center for Agricultural Publication and Documentation, Waginengen, The Netherlands, 239 pp.

Jones, B.F. (1986) Clay mineral diagenesis in lacustrine sediments. Pp. 291–300 in: *Studies in Diagenesis* (F.A. Mumpton, editor). *US Geological Survey Bulletin*, **1578**.

Jones, B.F. and Deocampo, D.M. (2003) Geochemistry of Saline Lakes. Pp. 393–424 in: *Surface and Ground Water, Weathering, and Soils* (J.I. Drever, editor). Treatise on Geochemistry, **5**. Elsevier, Amsterdam.

Jones, B.F. and Spencer, R.J. (1999) Clay mineral diagenesis at Great Salt Lake, Utah, USA. Pp. 293–297 in: *5th International Symposium on the Geochemistry of the Earth's Surface*.

Jones, B.F., Eugster, H.P., and Rettig, S.L. (1977) Hydrochemistry of the Lake Magadi basin, Kenya. *Geochimica et Cosmochimica Acta*, **41**, 53–72.

Kiage, L.M. and Liu, K.-B. (2006) Late Quaternary paleoenvironmental changes in East Africa: a review of multiproxy evidence from palynology, lake sediments, and associated records. *Progress in Physical Geography*, **30**, 633–658.

Koch, C. (1986) The vertebrate taphonomy and palaeoecology of the Olorgesailie Formation (Middle Pleistocene, Kenya), PhD dissertation, University of Toronto, Canada.

Langmuir, D. (1997) *Aqueous Environmental Geochemistry*, Prentice Hall, New Jersey, USA, 600 pp.

Larsen, D. (2008) Revisiting silicate authigenesis in the Pliocene-Pleistocene Lake Tecopa beds, southeastern California: Depositional and hydrological controls. *Geosphere*, **4**, 612–639.

Mahaney, W.C. (1991) Distributions of halloysite-metahalloysite and gibbsite in tropical mountain paleosols: relationship to Quaternary paleoclimate. *Palaeogeography, Palaeoclimatology, Palaeoecology*, **88**, 291–230.

Millot, G. (1964) *Geologie des argiles.* Masson et Cie, Paris.

Mizota, C., Kawasaki, I., and Wakatsuki, T. (1988) Clay mineralogy and chemistry of seven pedons formed in volcanic ash, Tanzania. *Geoderma*, **43**, 131–141.

Moore, D.M. and Reynolds, R.C. (1997) *X-ray Diffraction and the Identification and Analysis of Clay Minerals*. Oxford University Press, Oxford, UK.

National Academy of Sciences (2010) *Understanding climate's influence on human evolution.* National Academies Press, Washington, D.C.

Owen, R.B. and Renaut, R.W. (1981) Palaeoenvironments and sedimentology of the middle Pleistocene Olorgesailie Formation, southern Kenya Rift Valley. *Palaeoecology of Africa*, **13**, 147–174.

Owen, R.B., Potts, R., Behrensmeyer, A.K., and Ditchfield, P. (2008) Diatomaceous sediments and environmental change in the Pleistocene Olorgesailie Formation, southern Kenya Rift Valley. *Palaeogeography, Palaeoclimatology, Palaeoecology*, **269**, 17–37.

Potts, R. (1994) Variables versus models of early Pleistocene hominid land use. *Journal of Human Evolution*, **27**, 7–24.

Potts, R. (1989) Olorgesailie: New excavations and findings in Early and Middle Pleistocene contexts, southern Kenya rift valley. *Journal of Human Evolution*, **18**, 477–484.

Potts, R., Behrensmeyer, A.K., and Ditchfield, P. (1999) Paleolandscape variation and Early Pleistocene hominid activities: Members 1 and 7, Olorgesailie Formation, Kenya. *Journal of Human Evolution* **37**, 747–788.

Potts, R., Behrensmeyer, A.K., Deino, A., Ditchfield, P., and Clark, J. (2004) Small mid-Pleistocene hominin associated with east African Acheulean technology. *Science*, **305**, 75–78.

Retallack, G.J. (2001) *Soils of the Past, An Introduction to Paleopedology*. Unwin Hyman, Boston, USA.

Shackleton, R.M. (1978) A geological map of the Olorgesailie area. In: *Geological Background to Fossil Man*, map insert (W.W. Bishop, editor), Scottish Academic Press, Edinburgh.

Sheldon, N.D. and Tabor, N.J. (2009) Quantitative paleoenvironmental and paleoclimatic reconstruction using paleosols. *Earth Science Reviews*, **95**, 1–52.

Sikes, N.E., Potts, R., and Behrensmeyer, A.K. (1999) Early Pleistocene habitat in Member 1 Olorgesailie based on paleosol stable isotopes. *Journal of Human Evolution*, **37**, 721–746.

Singer, A., and Stoffers, P. (1980) Clay mineral diagenesis in two East-African Lake Sediments. *Clay Minerals*, **15**, 291–307.

Stoessell, R.K. (1988) 25ºC and 1 atm dissolution experiments of sepiolite and kerolite. *Geochimica et Cosmochimica Acta*, **52**, 365–374.

Stoessell, R.K. and Hay, R.L. (1978) The geochemical origin of sepiolite and kerolite at Amboseli, Kenya. *Contributions to Mineralogy and Petrology*, **65**, 255–267.

Tardy, Y., Cheverry, C., and Fritz, B. (1974) Neoformation d'une argile magnesienne dan les depressions interdunaires du lac Tchad: Application aux domaines de stabilite des phyllosilicates alumineaux mangesiens et ferrieres. *Comptes Rendu de l'Academie de Science Français, Paris, Serial C*, **278**, 1999–2002.

Trauth, M.H., Maslin, M.A., Deino, A., and Strecker, M.R. (2005) Late Cenozoic moisture history of East Africa. *Science*, **309**, 2051–2053.

Trueman, C.N., Behrensmeyer, A.K., Potts, R., and Tuross, N. (2006) High-resolution records of location and relative age from rare earth element chemistry of fossil bones. *Geochimica et Cosmochimica Acta*, **70**, 4343–4355.

USDA (1999) *Soil Taxonomy*. United States Department of Agriculture, Washington, DC, 871 pp.

(*Received 11 November 2009; revised 28 March 2010; Ms. 379; A.E. L.B. Williams*)